Active-Site Mutations of Diphtheria Toxin: Role of Tyrosine-65 in NAD Binding and ADP-Ribosylation†

Steven R. Blanke, Kathy Huang, and R. John Collier*

Department of Microbiology and Molecular Genetics, Harvard Medical School, and The Shipley Institute of Medicine, Boston, Massachusetts 02115

Received September 2, 1994; Revised Manuscript Received October 17, 1994®

ABSTRACT: Previous studies have suggested that tyrosine-65 (Tyr-65) of diphtheria toxin (DT) is located at the active site. To investigate the role of Tyr-65 in NAD binding and the ADP-ribosylation of elongation factor-2 (EF-2), we changed this residue to alanine and phenylalanine by site-directed mutagenesis of a synthetic gene encoding the catalytic fragment of DT (DTA). The alanine mutant was greatly diminished in ADP-ribosylation activity (350-fold) and NAD-glycohydrolase activity (88-fold), whereas the phenylalanine mutant was reduced in these activities only slightly. Dissociation constants (K_d) for NAD binding were 15 μM for wild-type DTA, 26 μM for the phenylalanine mutant, and greater than 800 μM NAD for the alanine mutant. However, both mutant enzymes were found to bind adenosine with nearly equal affinity as wild-type DTA. These results support a model of ADP-ribosylation in which the phenolic ring of Tyr-65 interacts with the nicotinamide ring of NAD, orienting the N-glycosidic bond of NAD for attack by the incoming nucleophile in a direct displacement mechanism.

A number of potent bacterial toxins, including diphtheria toxin (DT),[1] exotoxin A from *Pseudomonas aeruginosa* (ETA), pertussis toxin, cholera toxin, and heat-labile toxin from *Escherichia coli*, are proenzymes that are activated upon binding to and entering sensitive eukaryotic cells. In many toxins (including those listed above), the enzyme moiety catalyzes the ADP-ribosylation of a target protein, resulting in deleterious consequences to the intoxicated cell and/or animal host (Collier & Mekalanos, 1980; Moss & Vaughn, 1990). Despite the ability to distinguish their specific macromolecular targets, each of these enzymes may utilize a similar catalytic mechanism. We have studied the catalytic domain of DT as a model for understanding the active-site structure and function of the ADP-ribosyltransferases.

DT is organized into three distinct structural domains, which function directly in the three steps of intoxication: receptor binding, membrane translocation, and catalysis (Choe et al., 1992). After secretion from lysogenic strains of *Corynebacterium diphtheriae* carrying the phage-encoded *tox* gene, the toxin binds to the DT receptor by the carboxyl-terminal domain (R domain) and is internalized via receptor-mediated endocytosis (Naglich & Eidels, 1990; Naglich et al., 1992). Acidification of the endosomal compartment is believed to trigger a conformational change in the toxin, allowing the central domain (T domain) to insert into the endosomal membrane and the amino-terminal catalytic domain (C domain; equivalent to fragment A, or DTA) to be translocated across the membrane to the cytosol (Moskaug et al., 1991; Blewitt et al., 1985). Two processing events, proteolytic cleavage at Arg-193 and reduction of the disulfide linkage between cysteines-186 and -201, are required for release of DTA into the cytosol (Papini et al., 1993; Tsuneoka et al., 1993). Following these activation steps, DTA catalyzes transfer of the ADP-ribose moiety of NAD to a post-translationally modified histidine residue of elongation factor-2 (EF-2), called diphthamide (Van Ness et al., 1980). This covalent modification inactivates EF-2 and disrupts polypeptide chain elongation, resulting in cell death (Collier & Mekalanos, 1980; Collier, 1982; Collier & Traugh, 1969; Gill et al., 1969; Honjo et al., 1968).

Despite limited sequence homology among the ADP-ribosyltransferases, a number of important active-site residues have been discovered (Blanke et al., 1992). Glu-148 was identified as an active-site residue of DTA by photoaffinity labeling experiments with NAD and subsequent site-directed mutagenesis studies (Carroll et al., 1980; Carroll & Collier, 1984; 1985a; Tweten et al., 1985; Wilson et al., 1990). Analogous investigations with ETA revealed Glu-553 to be functionally homologous to Glu-148 of DT and provided an important reference point for identification of sequence homology between the catalytic domains of these toxins (Carroll & Collier, 1988). Among the residues of DT identified in sequence alignments, His-21 and Trp-50 have recently been shown to be important determinants for the binding of NAD (Blanke et al., 1994; Wilson et al., 1994).

In the investigations reported here, we have examined the function of Tyr-65 in DTA, which aligns with Tyr-481 in ETA. The crystal structures of these proteins reveal that these tyrosines are located in essentially identical positions within the active-site cleft of the catalytic domains (Choe et al., 1992; Allured et al., 1986). The importance of an active-site tyrosine in DTA had earlier been suggested when the

† The work was supported by NIH Grants AI-22021 and AI-22848, Postdoctoral Fellowship Award NIH8469 (S.R.B.), and NSF REU Grant BIO-9200321 (K. H.). This work was submitted by K.H. in partial fulfillment of a requirement for the Bachelor of Science Degree with Honors in Biology at Harvard University.

* Author to whom correspondence should be addressed.

® Abstract published in *Advance ACS Abstracts,* December 1, 1994.

[1] Abbreviations: ADP, adenosine diphosphate; BSA, bovine serum albumin; DT, diphtheria toxin; EF-2, elongation factor-2; DTA, diphtheria toxin fragment A; DTT, dithiothreitol; EDTA, ethylenediaminetetraacetic acid; ETA, exotoxin A; NAD, nicotinamide adenine dinucleotide; TCA, trichloroacetic acid; Tris, tris(hydroxymethyl)-aminomethane.

0006-2960/94/0433-15494$04.50/0

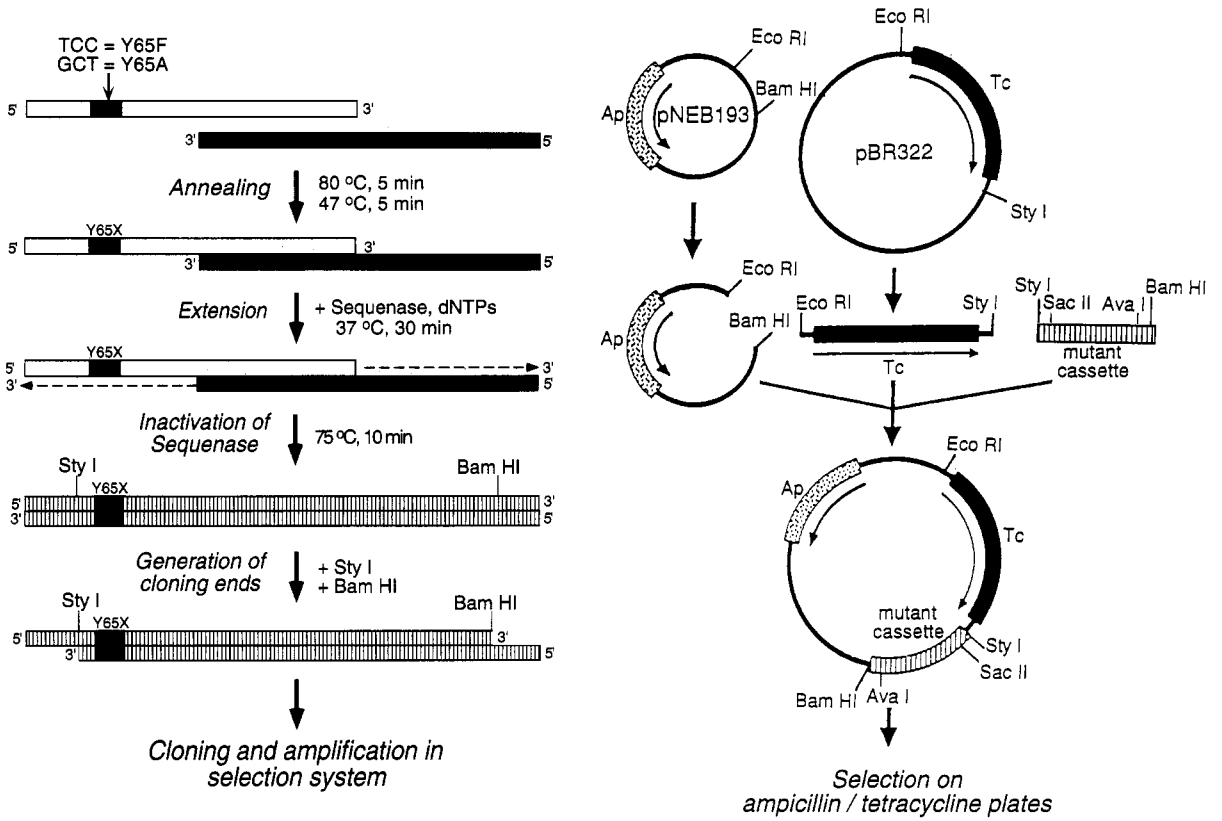

FIGURE 1: (A) Protocol for construction of mutations at residue 65. Synthetic cassettes were generated by annealing two self-priming oligonucleotides, extension of the strands with Sequenase version 2.0, and generation of the appropriate restriction sites by *Sty*I−*Bam*HI double digestions. The double digestion was allowed to proceed for 4.5 h, at which time the DNA was phenol extracted and ethanol precipitated in preparation for cloning. (B) A three-way directional-ligation was designed to allow for selection on ampicillin/tetracycline plates: The mutant cassettes were directly ligated with 200 ng of the *Eco*RI−*Bam*HI fragment of pBR322 encoding the tetracycline resistance gene, into the cloning vector pNEB193 at the *Eco*RI and *Sty*I sites. This construct was transformed into *E. coli* strain DH5. After selection on LB−ampicillin (100 mg/mL)/tetracycline (10 mg/mL) plates, two or three colonies were selected for sequencing to confirm the integrity of the synthetic cassettes.

toxin was inactivated by nitration with tetranitromethane of a single tyrosine in the catalytic domain (Beugnier & Zanen, 1977). In photolabeling studies with [2-^{3}H]8-azidoadenine and [2-^{3}H]8-azidoadenosine, DTA was modified specifically at Tyr-65 (Papini et al., 1991). This photolabeling reaction was inhibited equally well with nicotinamide as adenosine, suggesting that the nicotinamide ring of NAD may bind in close proximity to Tyr-65.

To pursue a more detailed understanding of the role of Tyr-65 in the ADP-ribosylation of EF-2, this residue was changed by site-directed mutagenesis to phenylalanine and alanine, using a recently completed synthetic gene encoding DTA (Blanke and Collier, unpublished data). Each of the DTA mutants, as well as wild-type enzyme, was overexpressed in *E. coli*, purified to near-homogeneity, and analyzed for ADP-ribosylation activity, NAD-glycohydrolase activity, and NAD binding. The results support a model in which Tyr-65 forms part of the nicotinamide subsite of the NAD binding pocket, and the hydrophobic phenol ring of Tyr-65 interacts with the nicotinamide ring in both the ground-state and transition-state complexes in the ADP-ribosylation of EF-2.

EXPERIMENTAL PROCEDURES

Reagents and Enzymes. All reagents were purchased from the following vendors: Restriction endonucleases, deoxyribonucleotides, and T4 DNA ligase from New England Biolabs; dideoxy sequencing kits from United States Biochemical; nickel chelate chromatography resin and plasmid purification columns from Qiagen, Inc.; [^{32}P]NAD (800 Ci/mmol) from Du Pont-New England Nuclear; [4-^{3}H]NAD (2.7 Ci/mmol) from Amersham; *E. coli* strain XL1-Blue from Stratagene; and pUC19 and pET-15b from New England Biolabs and Novagen Inc., respectively. Oligonucleotides encoding mutagenic codons at residue 65 were synthesized with an ABI Model 380A DNA synthesizer. The oligonucleotides were isolated with Oligonucleotide Purification Cartridges (Applied Biosystems), followed by further purification using denaturing polyacrylamide gel electrophoresis.

Recombinant DNA Procedures. Standard protocols were utilized for isolation of plasmid DNA, restriction endonuclease digestions, subcloning, and transformation of *E. coli* (Ausubel et al., 1987).

Design and Construction of Mutant Cassettes. The strategy for generating the site-directed mutations at residue 65 is outlined in Figure 1. All of the genetic manipulations were performed in a synthetic gene encoding the structural gene for DTA, maintained in pUC19 (replacing the *Kas*I−*Hin*dIII fragment, New England Biolabs) (Blanke and Collier, unpublished data). The synthetic gene was designed by altering the codon usage of the corynephage β gene to reflect the bias exhibited by highly expressed proteins in *E. coli*. The gene was divided into smaller, evenly-spaced fragments by engineering unique restriction sites throughout the open reading frame. The Tyr-65 mutations were encoded by synthetic cassettes, 67 base pairs in length, cloned into the

*Sac*II−*Ava*I sites of the synthetic gene, comprising bases 241−307. Each synthetic cassette was constructed by annealing a pair of oligonucleotides with complimentary sequences at the 3′ ends, to form a short duplex element of 15 base pairs. The annealed oligonucleotides served as both primer and template for strand extension with Sequenase, resulting in full length double-stranded cassettes. The *Sac*II−*Ava*I restriction sites were 9 base pairs from the end of each cassette.

The synthetic cassettes were generated by annealing 100 pmol of each purified oligonucleotide. The oligonucleotides were incubated for 5 min at 80 °C, followed by 5 min at 47 °C (Figure 1). The annealed strands were extended in a 30 μL reaction mixture of 5 mM dithiothreitol (DTT), 440 μM deoxynucleotides, and 50 μg/mL bovine serum albumin (BSA). The extension reactions were initiated by the addition of 13 units of Sequenase; reaction mixtures were incubated at 37 °C for 30 min, followed by incubation at 75 °C for 20 min. The mixture was diluted to 200 μL using water and restriction digestion buffer (New England Biolabs), and the appropriate restriction sites were generated by a *Sty*I−*Bam*HI double digestion for 4.5 h, followed by phenol extraction and ethanol precipitation. Half of this fragment preparation was ligated with 200 ng of the *Eco*RI−*Sty*I fragment excised from pBR322, encoding the tetracycline resistance gene, into the cloning vector pNEB193 (replacing the *Eco*RI−*Bam*HI sites). Following a 1 h ligation at 25 °C, the mixture was transformed into *E. coli* strain DH5. After selection for colonies possessing the insert on LB−ampicillin (100 μg/mL)/tetracycline (10 μg/mL) plates, the plasmids were amplified in liquid medium, and the cassettes were extracted by a 2 h restriction digest with *Sac*II−*Ava*I. The cassettes were then subcloned into the *Sac*II−*Ava*I sites of the synthetic gene maintained in pNEB193 or pET-15b. Plasmid DNA from transformed colonies was screened using Sequenase version 2.0, and those genes in pET-15b possessing the appropriate mutant codon 65 were transformed into the expression strain BL21(DE3).

Fermentation and Harvest of E. coli. A 50 mL culture of L-broth (100 μg/mL ampicillin) was inoculated with a single colony from an LB-amp plate freshly streaked with BL21(DE3) transformed with pET-15b-DTA. This inoculum was grown to an OD = 0.5 (600 nm) and then placed at 4 °C overnight. On the second day, 2 L baffled flasks, each containing 500 mL of L-broth (100 μg/mL ampicillin) prewarmed to 37 °C, were inoculated with 5 mL of the 50 mL overnight culture. The flasks were aerated on a rotary shaker at 37 °C. The cultures were induced at an OD_{600} = 1.0 with 1−2 mM isopropyl β-D-thiogalactopyranoside (IPTG). The cells were harvested after 1−2 h, immediately chilled to 4 °C, and centrifuged at 3000*g* for 10 min at 4 °C. The pellets were resuspended in 5 mL of ice cold sonication buffer, composed of 50 mM Na_2HPO_4, pH 8.0, 100 mM KCl, 0.1% Tween-20, 1.0 mM phenylmethanesulfonyl fluoride, and 20 mM β-mercaptoethanol. The resuspended pellets were either frozen at −70 °C or sonicated immediately.

Purification of Mutant Toxins. The combined pellets were sonicated three times on ice for 30−45 s, using a Sonifier Cell Disruptor 350 (Branson Sonic Power Co.), with the power control at 5 and the duty cycle at 40%. The extracts were chilled on ice for at least 1 min between each sonication cycle. Cellular debris was pelleted by centrifuging at 5000*g* for 30 min at 4 °C. The supernatants were collected and chilled, while the pellets were resuspended in 5−10 mL of sonication buffer and sonicated again as described above.

The synthetic gene encoding DTA was designed with a polyhistidine N-terminal fusion peptide, facilitating purification by nickel chelate affinity chromatography. The crude extracts were clarified immediately before chromatography by centrifuging at 20000*g* for 15 min. The extracts were loaded directly onto a 3−5 mL nickel chelate affinity column (Qiagen), pre-equilibrated with 10 bed volumes of sonication buffer. The column was washed with 5 bed volumes of sonication buffer plus 20 mM imidazole, followed by 2 bed volumes of 25 mM Tris-HCl, pH 8.0, plus 20 mM imidazole. The purified proteins were eluted with 5 bed volumes of 25 mM Tris-HCl, pH 8.0, plus 50 mM imidazole. The column fractions were analyzed by sodium dodecyl sulfate−polyacrylamide gel electrophoresis (SDS−PAGE), and the purified protein was pooled.

Proteolytic Removal of the Polyhistidine Fusion Peptide. Typically, 1.5 mg of protein in 20 mM Tris-HCl, pH 7.4, and 10 mM BME was incubated with 7.5 μg of bovine trypsin (Sigma) for 60 min on ice. The entire incubation mixture was loaded on a 1.0 mL nickel chelation affinity column to bind uncut DTA as well as the cleaved polyhistidine peptide. The flow-through fractions were collected and combined with two 1.0 mL washes of 20 mM Tris-HCl, pH 7.4, and 10 mM BME. This protein was further purified using anion exchange chromatography (FPLC Mono Q from Pharmacia). Side fractions were pooled, desalted, and repurified using anion exchange chromatography.

NAD:EF-2 ADP-Ribosyltransferase Assay. The NAD:EF-2 ADP-ribosyltransferase assay measures the initial rates of incorporation of the [^{32}P]NAD ADP-ribose moiety of NAD into the trichloroacetic acid (TCA)-precipitable EF-2 fraction of the reaction mixture. The assay was performed essentially as previously described (Blanke et al., 1994).

NAD-Glycohydrolase Assay. The initial rates of NAD-glycohydrolysis by DTA were determined by the hydrolysis of [*nicotinamide*-4-^{3}H]NAD, as previously described (Blanke et al., 1994).

Fluorescence Quenching. The determination of NAD binding by the quenching of intrinsic toxin fluorescence at pH 8.0 and 25 °C was performed as previously described (Wilson et al., 1990).

RESULTS

Production of Wild-Type and Mutant Proteins. Substitutions for Tyr-65 were generated by cloning synthetic mutant cassettes between the *Sac*II and *Ava*I sites of an entirely synthetic gene encoding DTA plus a 17 residue amino-terminal hexahistidine fusion peptide (Figure 1) (Blanke and Collier, unpublished results). Each gene encoding a mutant protein, cloned into *Nco*I−*Bam*HI sites of the expression vector pET-15b, was completely sequenced. The proteins were expressed in the *E. coli* strain BL21(DE3a) by activation of the T7 RNA polymerase with IPTG and were initially purified by nickel chelate chromatography. The amino-terminal hexahistidine fusion peptides were removed enzymatically with trypsin, and the authentic proteins were then further purified by anion exchange chromatography (FPLC). Protein purity was estimated by SDS−PAGE to be >99% for wild-type DTA, >95% for Y65A, and >90% for Y65F.

Table 1: Comparison of Specific Activities for ADP-Ribosyltransferase and NAD-Glycohydrolase Reactions by Wild-Type and Mutant DTA Enzymes

	ADP-ribosylation[a]		NAD-glycohydrolase[b]	
enzyme	sp act.[c]	rel act.	sp act.[d]	rel act.
wild type	660 ± 90	1.0 (1/1)	$(9.3 \pm 1.4) \times 10^{-3}$	1.0 (1/1)
Y65F	170 ± 20	0.26 (1/3.8)	$(13 \pm 1.6) \times 10^{-3}$	1.4 (1/0.72)
Y65A	1.9 ± 0.5	0.0029 (1/350)	$(0.11 \pm 0.0083) \times 10^{-3}$	0.011 (1/88)

[a] Assays were performed at 25 °C. Reaction mixtures contained 50 mM Tris-HCl, pH 8.0, 1 mM EDTA, 10 mM DTT, 50 μg/mL BSA, 2.0 μM EF-2, and 50 μM NAD. The values were calculated from at least two independent assays, each performed in duplicate. [b] Assays were performed at 25 °C: 50 mM Tris-HCl, pH 8.2, 1 mM EDTA, 5.0 mM DTT, 50 μg/mL BSA, and 50 μM NAD. The values were calculated from at least four independent assays, each performed in duplicate. [c] Defined as the number of moles of EF-2 ADP-ribosylated per minute per mole of enzyme. [d] Defined as the number of moles of NAD hydrolyzed per minute per mole of enzyme.

ADP-Ribosylation and NAD-Glycohydrolase Activities of Mutant Proteins. The effect of substitutions for Tyr-65 on ADP-ribosylation activity was estimated by measuring initial rates at 50 μM NAD and 2.0 μM EF-2, pH 8.0, and 25 °C (Table 1). The Y65F was only slightly reduced in ADP-ribosylation activity (ca. 4-fold), while the Y65A mutant was more drastically attenuated (350-fold).

In the absence of EF-2, DTA hydrolyzes NAD to nicotinamide and ADP-ribose at a slow but measurable rate, a reaction with no known physiological significance. Relative specific activities in the NAD-glycohydrolase reaction were determined from initial rates of [^{3}H]nicotinamide release, at 50 μM NAD, pH 8.0, and 25 °C (Table 1). Similar to the ADP-ribosylation reaction, the Y65A mutant was highly attenuated in NAD-glycohydrolase activity (88-fold), while the Y65F mutant exhibited activity essentially identical to that of wild-type enzyme.

Effects of Mutations on NAD Binding. The diminished ADP-ribosylation and NAD-glycohydrolase activities of the Y65A mutant suggested that NAD binding had been altered. The dissociation constants (K_d) of NAD binding were measured by quenching of intrinsic protein fluorescence at pH 8.0 and 25 °C (Wilson et al., 1990). Substituting alanine for Tyr-65 greatly reduced the ability of DTA to bind NAD, while the phenylalanine mutant was similar to wild-type DTA (Figure 2). The K_d for NAD binding to Y65F was 26 μM, compared to 15 μM for wild-type DTA (Table 2). The K_d value for Y65A could not be accurately measured, as there was minimal quenching of intrinsic protein fluorescence, even up to 1 mM NAD, indicating that the substrate bound poorly to this mutant enzyme. The binding energies for NAD in the ground-state binary complex were calculated from the dissociation constants, according to the equation:

$$\Delta G_s = RT \ln K_d$$

The ground-state binding energy was only 0.3 kcal/mol higher for the Y65F mutant (−6.3 kcal/mol) compared to that of wild-type DTA (−6.6 kcal/mol), while the difference in binding energy of the Y65A mutants was estimated to be greater than 3 kcal/mol (Table 2).

Effects of Mutations on Adenosine Binding. In previous studies, it had been demonstrated that adenosine binds to DTA with lower affinity than NAD (Kandel et al., 1974). Binding constants were found to be 320 μM, 370 μM, and 270 μM, as determined, respectively, by half-maximal inhibition of ADP-ribosylation, half-maximal inhibition of NAD-glycohydrolase, and dynamic dialysis. In these investigations, we found that intrinsic protein fluorescence was quenched up to 40% percent when wild-type DTA was titrated with concentrations of adenosine ranging from 50 μM to 1.40 mM. Hanes−Woolf analysis of these data yielded a K_d value of 320 μM (Table 3), in good agreement with previous studies (Kandel et al., 1974). Analysis of the

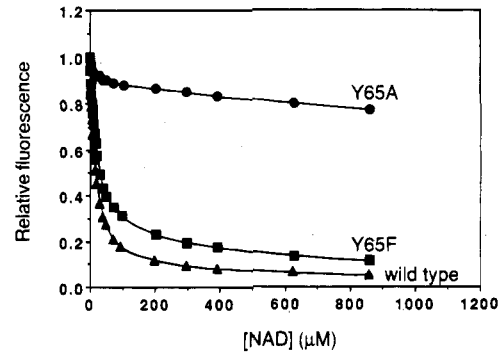

FIGURE 2: Quenching of intrinsic protein fluorescence for DTA-WT, DTA-Y65F, and DTA-Y65A by NAD. The assays were performed as previously described (Wilson et al., 1990), by titrating with NAD at 25 °C. The plots are from single fluorescence quenching experiments, which were repeated at least three times. The percent quenching at each NAD concentration was calculated from the data and analyzed by Hanes plots to determine the dissociation constants for the wild-type and mutant proteins. The K_d values are summarized in Table 2.

Table 2: Comparison of Dissociation Constants and Binding Energies for NAD Binding to Wild-Type and Mutant DTA Enzymes[a]

enzyme	K_d (μM)[b]	difference in binding energies ($\Delta\Delta G_s$, kcal/mol)[c]7
wild type	15 ± 1	
Y65F	26 ± 2	+0.32
Y65A	>800[d]	>3[e]

[a] Assays were performed at 25 °C. Intensity of fluorescence emission was measured over the range of 315−400 nm with excitation at 295 nm. The values were generated from the average of at least three independent assays. [b] Determined from Hanes−Woolf analysis of the percentage of fluorescence quenching as a function of NAD concentration. [c] Determined from the difference in the Gibbs free energy $\Delta G_s = RT \ln K_d$, obtained for NAD binding to the wild-type and mutant DTA. [d] Estimated from the observation that <20% of the fluorescence was quenched at NAD concentrations of up to 910 μM. [e] Estimated from the observation in footnote *d*, indicating that the K_d value for NAD binding must be >800 μM.

Table 3: Comparison of Dissociation Constants and Binding Energies for Adenosine Binding to Wild-Type and Mutant DTA Enzymes[a]

enzyme	K_d (μM)[b]	difference in binding energies ($\Delta\Delta G_s$, kcal/mol)[c]
wild type	320 ± 70	
Y65F	320 ± 8	−0.01
Y65A	230 ± 20	−0.20

[a] Assays were performed at 25 °C. Intensity of fluorescence emission was measured over the range of 315−400 nm with excitation at 295 nm. The values were generated from the average of at least two independent assays. [b] Determined from Hanes−Woolf analysis of the percentage of fluorescence quenching as a function of adenosine concentration. [c] Determined from the difference in the Gibbs free energy $\Delta G_s = RT \ln K_d$, obtained for adenosine binding to the wild-type and mutant DTA.

Table 4: Kinetics of ADP-Ribosyltransferase Reaction[a]

enzyme	K_m [NAD] (μM)	k_{cat} (min^{-1})	k_{cat}/K_m (M^{-1} min^{-1})	rel k_{cat}/K_m	$\Delta G_{apparent}$ (kcal/mol)[b]
wild type	40 ± 2.4	1200 ± 180	3.0×10^7	1.0 (1/1)	
Y65F	9.5 ± 0.33	250 ± 80	2.6×10^7	0.86 (1/1.2)	+0.086
Y65A	220 ± 59	10 ± 3.0	4.5×10^4	0.0015 (1/670)	+3.9

[a] The kinetic parameters were determined from Lineweaver–Burk plots of initial rates of reaction as a function of NAD concentration at 2.0 μM EF-2. The values were calculated from the average of at least 3 assays, each performed in duplicate. [b] Determined from the $\Delta G = -RT \ln[(k_{cat}/K_m)_{mutant}/(k_{cat}/K_m)_{wildtype}]$.

mutant proteins revealed that Y65F binds adenosine with equal affinity to wild-type DTA (320 μM). However, although Y65A was greatly attenuated in NAD binding, this mutant protein had slightly higher affinity for adenosine (230 μM) than wild-type protein.

Kinetic Studies. The kinetic parameters for initial rates of ADP-ribosyltransferase activity were determined from Lineweaver–Burk plots of initial rates as a function of NAD concentration (Table 4). The Michaelis constant (apparent K_m) for Y65F was determined to be 9.5 μM, well below the value of 40 μM for wild-type DTA. The turnover number, k_{cat}, was reduced (250 min^{-1}) compared to that of wild-type enzyme (1200 min^{-1}). For Y65A, the apparent K_m was 220 μM, while k_{cat} was reduced substantially to 10 min^{-1}. The catalytic efficiency (k_{cat}/K_m) for Y65F was nearly identical to that for wild-type DTA, but was reduced by a factor of approximately 670 for Y65A.

The change in apparent binding energy (ΔG) from mutating residues that interact with the transition-state intermediate of the ADP-ribosylation reaction can be determined from the ratio of k_{cat}/K_m (Wilkinson et al., 1983; Carter et al., 1984; Fersht, 1987a), with

$$\Delta G = -RT \ln[(k_{cat}/K_m)_{mutant}/(k_{cat}/K_m)_{wildtype}]$$

The apparent free energy change from substituting alanine for tyrosine was +3.9 kcal/mol, while the apparent change from substituting phenylalanine for tyrosine was only +0.086 kcal/mol (Table 4).

Kinetic parameters were also determined from the initial rates of NAD-glycohydrolase activity as a function of NAD concentration, and the results of Lineweaver–Burk analysis are displayed in Table 5. The K_m value of Y65F was twice that of wild type, but the turnover number (k_{cat}) was also approximately twice that of wild-type DTA. Thus, catalytic efficiency was almost identical in the two proteins. In contrast, the K_m value calculated for Y65A was markedly increased, by nearly 200-fold, and k_{cat} was essentially the same, at 0.020 min^{-1}, as compared with 0.015 min^{-1} for wild type. Consequently, the catalytic efficiency was reduced by approximately 140-fold for this mutant. The apparent free energy change from substituting phenylalanine for tyrosine in the NAD-glycohydrolase reaction was only +0.05 kcal/mol, while the change from substituting alanine for tyrosine was +2.9 kcal/mol.

DISCUSSION

Although crystallographic studies of NAD binding have not yet yielded a model of this dinucleotide in the active-site cleft of DT (or of any other ADP-ribosyltransferase), various data suggest that Tyr-65, along with His-21 and Glu-148, forms part of the nicotinamide subsite (Blanke et al., 1992). In an early model of NAD binding to the active-site cleft of ETA, proposed by Brandhuber et al. (1988), the nicotinamide ring was hypothesized to interact with the side chain of Trp-466 (corresponding to Trp-50 in DT), while the adenine ring stacks against the phenolic ring of Tyr-481 (corresponding to Tyr-65 of DT). However, this organization of the active site was inconsistent with the results of experiments by Carroll and co-workers (Carroll & Collier, 1984; Carroll et al., 1985a,b) in which NAD was used as a photoaffinity label with DT or ETA. The structure of the photoproduct formed, which features the entire nicotinamide moiety of NAD covalently linked through C-6 to the decarboxylated γ-methylene carbon of Glu-148 in DT, suggested that the side chain of this moiety must be in close proximity to the N-glycosidic bond cleaved during the ADP-ribosylation and NAD-glycohydrolase reactions. Subsequently, the photolabeling studies by Papini et al. (1991) with 8-azidoadenine and 8-azidoadenosine led the authors to suggest a model in which NAD assumed effectively the opposite orientation—with the nicotinamide ring stacked onto the phenolic ring of Tyr-65 and the adenine ring on Trp-50. This proposal is strengthened by our discovery that Y65A, which is severely attenuated in NAD binding, is able to bind adenosine with approximately the same affinity as wild-type DTA. These findings suggest that Tyr-65 does not interact with the adenine or adenine ribose moieties of NAD. Besides being more consistent with the photoinduced linking of nicotinamide to Glu-148, this model is supported by the crystallographic structure of DT, in which the endogenous dinucleotide, adenylyl-3′,5′-uridine monophosphate (ApUp), binds tightly (and competitively with NAD) to the active site of DT (Choe et al., 1992). The uridine ring of ApUp, which may be considered an analog of the nicotinamide ring of NAD, is positioned in a pocket between the imidazole ring of His-21 and the phenolic ring of Tyr-65. It is thus a reasonable assumption that the nicotinamide ring of NAD binds in approximately the same location, and therefore in close proximity to the phenolic ring of Tyr-65.

The fact that phenylalanine, but not alanine, can effectively substitute for Tyr-65 in both NAD and catalysis suggests that it is primarily the aromatic phenol ring of Tyr-65 that is important for interacting with the heteroaromatic nicotinamide ring. The involvement of tyrosine residues in hydrophobic and aromatic–aromatic interactions with substrates and inhibitors has been well documented. Mutagenesis studies and/or X-ray crystallographic analysis has shown tyrosine to be a major determinant of binding specificity in human lysozyme (Muraki et al., 1992), *E. coli* ATP-synthase (Wise, 1990), α-amylase from Saccharomycopsis (Matsui et al., 1994), the binding site of p11 for annexin II (Kube et al., 1992), the binding of epidermal growth factor with its receptor (Campion et al., 1990), and the binding of the nicotinic acetylcholine receptor with the competitive antagonist curare (Filatov et al., 1993). Although such detailed interaction geometry as dihedral angles and aromatic ring center-to-center separation between Tyr-65 and the nicotinamide ring of NAD must await a structure determination with bound substrate, the experimental results support a model of aromatic–aromatic interactions between these two moieties.

If this model is correct, interaction with Tyr-65 may serve to orient the nicotinamide ring and the nicotinamide–ribose

Table 5: Kinetics of NAD-Glycohydrolase Reaction[a]

enzyme	K_m (NAD) (μM)	k_{cat} (min^{-1})	k_{cat}/K_m (M^{-1} min^{-1})	rel k_{cat}/K_m	$\Delta G_{apparent}$ (kcal/mol)[b]
wild type	$(2.0 \pm 0.5) \times 10$	$(1.5 \pm 0.3) \times 10^{-2}$	750	1.0 (1/1)	
Y65F	$(3.9 \pm 0.4) \times 10$	$(2.7 \pm 0.1) \times 10^{-2}$	690	0.92 (1/1.1)	+0.049
Y65A	$(3.7 \pm 2.9) \times 10^3$	$(2.0 \pm 0.4) \times 10^{-2}$	5.4	0.0072 (1/140)	+2.9

[a] The kinetic parameters were determined from Lineweaver–Burk plots of initial rates of reaction as a function of NAD concentration. The values were calculated from the average of at least two assays performed in duplicate. [b] Determined from $\Delta G = -RT \ln[(k_{cat}/K_m)_{mutant}/(k_{cat}/K_m)_{wildtype}]$.

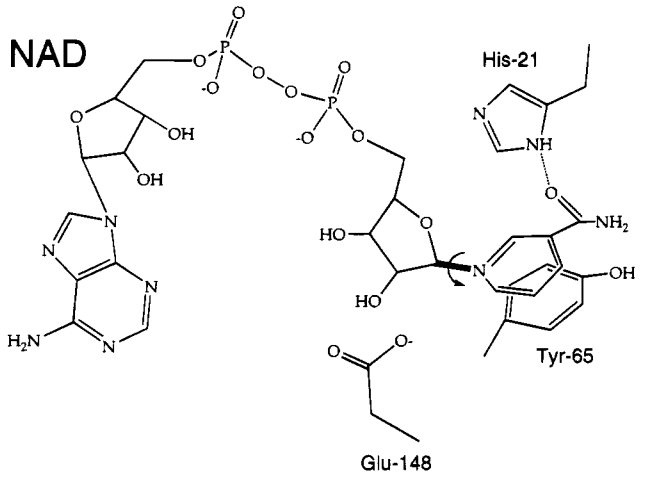

FIGURE 3: Model of how Tyr-65 and His-21 interact with the nicotinamide ring of NAD. These investigations revealed that it is the phenol ring of Tyr-65, and not the phenolic hydroxyl group, that is important for interacting with NAD. In particular, we propose that Tyr-65 orients the nicotinamide ring by aromatic interactions, while previous work suggests that His-21 further orients this ring by formation of a hydrogen bond with the nicotinamide carboxyamide moiety of NAD (Blanke et al., 1994). These interactions are important for limiting the rotational degrees of freedom of the N-glycosidic bond of NAD, and thus orienting this bond for nucleophilic attack by diphthamide.

linkage of NAD in the active site of DTA. Although this bond is highly activated for hydrolysis ($\Delta G = 8.2$ kcal/mol) (Zatman et al., 1953), there is considerable rotational freedom of the nicotinamide ring around the N-glycosidic bond relative to the adjacent ribose ring. The ADP-ribosylation reaction has been proposed to proceed by a direct displacement reaction, with the π-imidazole nitrogen of diphthamide being activated by Glu-148 for nucleophilic attack on the N-glycosidic bond of NAD (Wilson et al., 1990; Wilson & Collier, 1992). The structure of EF-2 has not yet been solved, but it is conceivable that the large size of this protein (100 kDa) restricts the extent to which diphthamide can extend into the NAD binding pocket of DTA. The hydrophobic interaction of the nicotinamide ring with the phenolic side chain of Tyr-65, coupled with the hydrogen bonding interaction with the imidazole ring of His-21 (Blanke et al., 1994), may serve to limit both rotational and translational freedom of the N-glycosidic bond and provide for a more favorable orientation for nucleophilic attack (Figure 3).

Kinetic analysis revealed that the alanine substitution (Y65A) destabilizes the transition state by 3.9 kcal/mol. This is a higher value than the 1.0–2.5 kcal/mol predicted for the loss of stabilizing energy provided by the interaction of an aromatic protein residue with the aromatic moieties of substrates (Burley & Petsko, 1985, 1988) and may well reflect the effects of structural perturbations in the active site. Removal of the planar phenolic ring creates a hole in the active site, which can lead to rearrangements in local solvent and side chain structures. These rearrangements can induce changes in local substrate conformation which have profound effects on the electronic nature of the transition state (Horenstein & Schramm, 1993; Fersht, 1987b) and can influence the developing charge distribution for stabilization of the transition state (Horenstein & Schramm, 1993; Fersht, 1987b; Venanzi et al., 1992; Sjoberg & Politzer, 1990; Lamotte-Brasseur et al., 1990). By comparison, mutating Tyr-65 to phenylalanine (Y65F) only slightly destabilized the transition state (0.086 kcal/mol). The removal of the phenolic hydroxyl group may disrupt a hydrogen bond to the transition-state intermediate, although the binding energy contribution of a single hydrogen bond by an uncharged residue has been estimated to stabilize the transition state of an enzyme-catalyzed reaction by a slightly higher value (0.5–1.8 kcal/mol) (Fersht et al., 1985; Fersht, 1987b). Interestingly, while the apparent K_m for Y65F was slightly lower than that for wild-type enzyme, this enzyme was still slightly attenuated in catalytic efficiency (k_{cat}/K_m). This result suggests that, for the ADP-ribosylation of EF-2, the more hydrophobic phenylalanine ring at residue 65 has slightly higher affinity for NAD, but the phenolic hydroxyl group of tyrosine at this position may play a role in stabilizing the developing transition state.

In the NAD-glycohydrolase reaction, kinetic analysis indicated that both the phenylalanine and alanine substitutions for Tyr-65 resulted in attenuated affinity for NAD (ca. 2- and 200-fold lower K_m values, respectively). However, in contrast to the DTA-catalyzed ADP-ribosylation of EF-2, neither of these substitutions had an effect on enzyme turnover (k_{cat}). These results support a model for the glycohydrolytic reaction in which, subsequent to binding NAD, DTA destabilizes the ground-state complex to an oxycarbonium transition state in an S_N1 type reaction.

A previous study showed that a phenylalanine substitution for Tyr-481 in ETA, which is homologous to Tyr-65 of DT by sequence comparison and X-ray crystallography, reduced ADP-ribosylation activity relative to wild-type activity in crude *E. coli* extracts (Lukac & Collier, 1988) However, no conclusions could be drawn as to whether the phenolic ring of Tyr-481 was important for NAD binding and catalysis. Sequence and/or structural alignments with other ADP-ribosylating toxins suggest that the homologues for Tyr-65 are Phe-96 in pertussis toxin, Phe-94 in cholera toxin, and Phe-94 in heat-labile toxin from *E. coli*. Consistent with our findings, this suggests that, among the ADP-ribosylating toxins, either a tyrosine or a phenylalanine in this position can serve a similar function. These results may have direct relevance to the expanding class of enzymes that catalyze ADP-ribosylation reactions, which not only includes many bacterial exotoxins, but also other enzymes of prokaryotic and eukaryotic origin. For instance, Tyr-907 of human poly(ADP-ribose) polymerase was recently identified as a ho-

mologue of Tyr-65 by sequence alignments (Marsischky et al., 1994). Identification of these conserved active-site features provides the groundwork for construction of genetically attenuated toxoids to be used in recombinant vaccines, as well as rational inhibitor design for the larger family of ADP-ribosyltransferases.

ACKNOWLEDGMENT

The authors would like to acknowledge Angela Vilche for excellent technical assistance.

REFERENCES

Allured, V. S., Collier, R. J., Carroll, S. F., & McKay, D. B. (1986) *Proc. Natl. Acad. Sci. U.S.A. 83*, 1320.

Ausubel, F., Brent, R., Kingston, R. E., Moore, D. D., Seidman, J. G., Smith, J. A., & Struhl, K. (1987) in *Current Protocols in Molecular Biology*, John Wiley and Sons, New York.

Beugnier, N., & Zanen, J. (1977) *Biochim. Biophys. Acta 490*, 225.

Blanke, S. R., Collier, R. J., Covacci, A., Fu, H., Killeen, K., Montecucco, C., Papini, E., Rappuoli, R., & Wilson, B. A. (1992) in *Bacterial Protein Toxins, Fifth European Workshop* (Witholt, B., Alouf, J. E., Boulnois, G. J., Cossart, P., Dijkstra, B. W., Falmagne, P., Fehrenbach, F. J., Freer, J., Niemann, H., Rappuoli, R., & Wadstrom, T., Eds.) pp 349−354, Gustav Fischer Verlag, New York.

Blanke, S. R., Huang, K., Wilson, B. A., Papini, E., Covacci, A., & Collier, R. J. (1994) *Biochemistry 33*, 5155.

Blewitt, M. G., Chung, L. A., & London, E. (1985) *Biochemistry 24*, 5458.

Brandhuber, B. J., Allured, V. S., Falbel, T. G., & McKay, D. B. (1988) *Proteins 3*, 146.

Burley, S. K., & Petsko, G. A. (1985) *Science 229*, 23.

Burley, S. K., & Petsko, G. A. (1988) *Adv. Protein Chem. 39*, 125.

Campion, S. R., Matsunami, R. K., Engler, D. A., & Niyogi, S. K. (1990) *Biochemistry 29*, 9988−9993.

Carroll, S. F., & Collier, R. J. (1984) *Proc. Natl. Acad. Sci. U.S.A. 81*, 3307.

Carroll, S. F., & Collier, R. J. (1988) *Mol. Microbiol. 2*, 293.

Carroll, S. F., Lory, S., & Collier, R. J. (1980) *J. Biol. Chem. 255*, 12020.

Carroll, S. F., McCloskey, J. A., Crain, P. F., Oppenheimer, N. J., Marschner, T. M., & Collier, R. J. (1985a) *Proc. Natl. Acad. Sci. U.S.A. 82*, 7237.

Carroll, S. F., Oppenheimer, N. J., Marschner, T. M., McCloskey, J. A., Crain, P. F., & Collier, R. J. (1985b) in *ADP-Ribosylation of Proteins* (Althaus, F. R., Hilz, H., & Shall, S., Eds.) pp 544−550, Springer-Verlag, New York.

Carter, P. J., Winter, G., Wilkinson, A. J., & Fersht, A. R. (1984) *Cell 38*, 835.

Choe, S., Bennett, M., Fujii, G., Curmi, P. M. G., Kantardjieff, K. A., Collier, R. J., & Eisenberg, D. (1992) *Nature 357*, 216.

Collier, R. J. (1982) in *ADP-Ribosylation Reactions* (Hayaishi, O., & Ueda, K., Eds.) pp 575−592, Academic Press, New York.

Collier, R. J., & Traugh, J. A. (1969) *Cold Spring Harbor Symp. Quant. Biol. 34*, 589.

Collier, R. J., & Mekalanos, J. J. (1980) in *Multifunctional Proteins* (Bisswanger, H., & Schmincke-Ott, E., Eds.) pp 261−291, John Wiley & Sons, New York.

Fersht, A. R. (1987a) *Biochemistry 27*, 1577.

Fersht, A. R. (1987b) *Trends Biochem. Sci. 12*, 301.

Fersht, A. R., Shi, J. P., Knill-Jones, J., Lowe, D. M., Wilkinson, A. J., Blow, D. M., Brick, P., Carter, P., Waye, M. M., & Winter, G. (1985) *Nature 314*, 235.

Filatov, G. N., Aylwin, M. L., & White, M. M. (1993) *Mol. Pharmacol. 44*, 237−241.

Gill, D. M., Pappenheimer, A. M., & Baseman, J. B. (1969) *Cold Spring Harbor Symp. Quant. Biol. 34*, 595.

Honjo, T., Nishizuka, Y., & Hayaishi, O. (1968) *J. Biol. Chem. 243*, 3553.

Horenstein, B. A., & Schramm, V. L. (1993) *Biochemistry 32*, 7089.

Kandel, J., Collier, R. J., & Chung, D. W. (1974) *J. Biol. Chem. 249*, 2088.

Kube, E., Becker, T., Weber, K., & Gerke, V. (1992) *J. Biol. Chem. 267*, 14175−14182.

Lamotte-Brasseur, J., Dive, G., Dehareng, D., & Ghuysen, J. M. (1990) *J. Theor. Biol. 145*, 183.

Lukac, M., & Collier, R. J. (1988) *J. Biol. Chem. 263*, 6146.

Marsischky, G. T., Wilson, B. A., & Collier, R. J. (1994) *J. Biol. Chem.* (submitted for publication).

Matsui, I., Yoneda, S., Ishikawa, K., Miyairi, S., Fukui, S., Umeyama, H., & Honda, K. (1994) *Biochemistry 33*, 451−458.

Moskaug, J. O., Stenmark, H., & Olsnes, S. (1991) *J. Biol. Chem. 266*, 2652.

Moss, J., & Vaughn, M. (1990) in *ADP-Ribosylating Toxins and G Proteins: Insights into Signal Transduction*, Library of Congress, Washington, DC.

Muraki, M., Harata, K., & Jigami, Y. (1992) *Biochemistry 31*, 9212−9219.

Naglich, J. G., & Eidels, L. (1990) *Proc. Natl. Acad. Sci. U.S.A. 87*, 7250.

Naglich, J. G., Metherall, J. E., Russell, D. W., & Eidels, L. (1992) *Cell 69*, 1051.

Papini, E., Santucci, A., Schiavo, G., Domenighini, M., Neri, P., Rappuoli, R., & Montecucco, C. (1991) *J. Biol. Chem. 266*, 2494.

Papini, E., Rappuoli, R., Murgia, M., & Montecucco, C. (1993) *J. Biol. Chem. 268*, 1567.

Sjoberg, P., & Politzer, P. (1990) *J. Phys. Chem. 94*, 3959.

Tsuneoka, M., Nakayama, K., Hatsuzawa, K., Komada, M., Kitamura, N., & Mekada, E. (1993) *J. Biol. Chem. 268*, 26461.

Tweten, R. K., Barbieri, J. T., & Collier, R. J. (1985) *J. Biol. Chem. 260*, 10392.

Van Ness, B. G., Howard, J. B., & Bodley, J. W. (1980) *J. Biol. Chem. 255*, 10710.

Venanzi, C. A., Plant, C., & Venanzi, T. J. (1992) *J. Med. Chem. 35*, 1643.

Wilkinson, A. J., Fersht, A. R., Blow, D. M., & Winter, G. (1983) *Biochemistry 22*, 3581.

Wilson, B. A., & Collier, R. J. (1992) *Curr. Top. Microbiol. Immunol. 175*, 27−41.

Wilson, B. A., Reich, K. A., Weinstein, B. R., & Collier, R. J. (1990) *Biochemistry 29*, 8643.

Wilson, B. A., Blanke, S. R., Reich, K. A., & Collier, R. J. (1994) *J. Biol. Chem.* (in press).

Wise, J. G. (1990) *J. Biol. Chem. 265*, 10403−10409.

Zatman, L., Kaplan, N., & Colowick, S. (1953) *J. Biol. Chem. 200*, 197.